RSC Advances

ROYAL SOCIETY
OF CHEMISTRY

www.rsc.org/advances

Dye-Sensitization of Boron-Doped Diamond Foam: Champion Photoelectrochemical Performance of Diamond Electrodes under Solar Light Illumination

Hana Krysova[1], Ladislav Kavan[1*], Zuzana Vlckova Zivcova[1], Weng Siang Yeap[2], Pieter Verstappen[2], Wouter Maes[2,3], Ken Haenen[2,3], Fang Gao[4] and Christoph E. Nebel[4]

[1]J. Heyrovsky Institute of Physical Chemistry of the AS CR, v.v.i., Dolejškova 3, CZ-182 23, Prague 8, Czech Republic

[2]Hasselt University, Institute for Materials Research (IMO), B-3590 Diepenbeek, Belgium

[3]IMEC vzw, IMOMEC, B-3590 Diepenbeek, Belgium

[4]Fraunhofer Institute for Applied Solid State Physics (IAF), Tullastrasse 72, D-79108 Freiburg, Germany

*To whom correspondence should be addressed. Tel.: +420 2 6605 3975; fax: +420 2 8658 2307; E-mail address: kavan@jh-inst.cas.cz

ABSTRACT. Diamond foams composed of hollow spheres of polycrystalline boron-doped diamond are chemically modified with two donor-acceptor type molecular dyes, **BT-Rho** and **CPDT-Fur**, and tested as electrode materials for p-type dye-sensitized solar cells with an aqueous electrolyte solution containing methyl viologen as a redox mediator. Reference experiments with flat polycrystalline diamond electrodes evidence full blocking of the methyl viologen redox reaction by these dyes, whereas only partial blocking is observed for the diamond foams. This is ascribed to sp^2-carbon impurities in the foam, viz. *trans*-polyacetylene and graphite-like carbon. Cathodic photocurrents under solar light illumination are about 3 times larger on foam electrodes compared to flat diamond. Long-term (1-2 days) illumination of the sensitized foam electrodes with chopped light at 1 sun intensity causes an increase of the cathodic photocurrent density to ca. 15-22 μA/cm^2. These photocurrent densities represent the largest values reported so far for dye-sensitized diamond electrodes. The photoelectrochemical activation of the sensitized diamond electrodes is accompanied with characteristic changes of the dark voltammogram of the MV^{2+}/MV^+ redox couple and with gradual changes of the IPCE spectra.

1

1. INTRODUCTION

Dye-sensitized solar cells (DSCs) also called Graetzel cells,[1] are based on spectral sensitization of wide-band gap semiconductor electrodes to visible light. The most successful device so far, employing an n-TiO_2 photoanode, achieved 13 % solar power conversion efficiency.[2] A mirror alternative of this solar cell uses a dye-sensitized photocathode, such as p-NiO. However, the efficiency of such p-DSCs is still by a factor of 10 smaller[3,4] and the same holds for tandem devices (p,n-DSC) in which both electrodes are made from dye-sensitized semiconductors.[5] The optimization of photocathodes in p-DSCs remains, therefore, an open research area. Previous studies pointed on B-doped nanocrystalline diamond (BDD) to be a promising replacement of p-NiO. Diamond electrodes outperform p-NiO in chemical and electrochemical stability,[6,7] optical transparency[8,9] and hole diffusion coefficient (2-30 cm^2/s)[10] (cf. the value for p-NiO being $4 \cdot 10^{-8}$ cm^2/s).[11] Nevertheless, the reported photoelectrochemical performance of p-BDD is not satisfying yet. Under 1 sun illumination (AM1.5G; 100 mW/cm^2) a sensitized p-NiO can deliver short-circuit photocurrent densities of ca. 5 mA/cm^2, whereas the p-BDD electrodes provided photocurrent densities by 3 orders of magnitude lower, in the best case.[9]
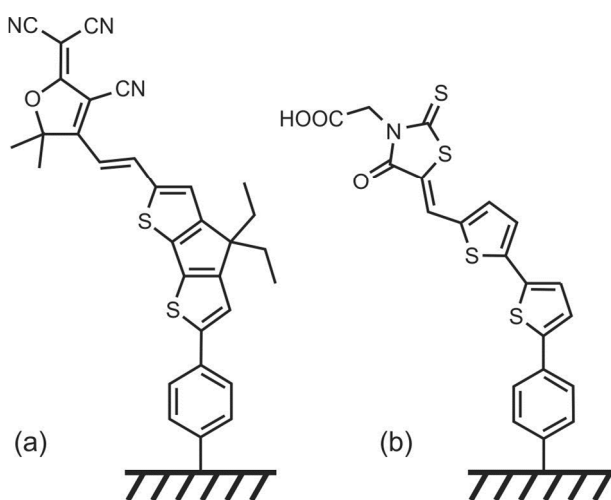
Spectral sensitization of diamond surfaces by organic dyes, absorbing visible light, has been pioneered in 2008 by Zhong et al.[12] who covalently anchored dicyanovinyl-bithophene and C_{60}-bithophene on H-terminated BDD through Suzuki cross-coupling reactions. They observed photocurrent densities of ca. 120 nA/cm^2 under white light illumination (150 W halogen lamp) in an aqueous electrolyte solution with methyl viologen acting as the electron carrier. Later on, photocurrent densities of ca. 4-6 μA/cm^2 were observed in similar systems under 1 sun illumination.[9] Sensitization of BDD by manganese phthalocyanine[13,14] or Ru(SCN)$_2$(pbca)$_2$ (pbca = 2,2'-bipyridine-4,4'-dicarboxylate) (commonly known as the N3 dye)[15] provided rather low photocurrent densities, typically of the order of 1-10 nA/cm^2 under white light illumination with an intensity of about 1 sun. Krysova et al.[16] reported on non-covalent anchoring of the 4-(bis{4-[5-(2,2-dicyanovinyl)thiophene-2-yl]phenyl}amino)benzoic acid dye (coded P1) through a polyethyleneimine linker. Although the P1 dye is known to be successful for the sensitization of p-NiO,[17,18] the reported photocurrent densities on diamond electrodes were again low, about 100-150 nA/cm^2 at white light intensity of 18 mW/cm^2. (Interestingly, the P1 dye turned out to be

2

appropriate for the sensitization of n-TiO_2, too,[18] which is reminiscent of the applicability of the N3 dye in both TiO_2 and diamond electrodes.[15]) Yeap et al.[19] modified the diamond surface with different thiophene-based molecular wires through a combination of diazonium electrografting and Suzuki cross-coupling, and observed photocurrent densities of ca. 150 nA/cm^2 under white light illumination (15 mW/cm^2 intensity).

One of the reasons for the poor photoelectrochemical performance of sensitized diamond is obviously the low surface area (roughness factor) and the lack of mesoporous texture of the BDD films applied so far.[16,19] The light-harvesting efficiency of a monolayer of dye molecules on a flat surface is inherently small. For instance, the maximum incident photon-to-electron conversion efficiency (IPCE) of the N3-dye monolayer on an atomically flat TiO_2 anatase is theoretically 0.27 % (and experimentally around 0.11 %)[20,21] while IPCEs exceeding 90% are commonly observed for a properly nanostructured anatase with a roughness factor of ca. 1000 (the roughness factor, R_f, being defined as the ratio of the physical surface area to the geometric electrode area)[1]. This finding raises the challenge to reproduce surface nanostructuring on diamond electrodes for p-DSC applications, too. The growth of nano-textured mesoporous diamond films has been attempted in the past by various protocols, such as inductively-coupled plasma etching,[22,23] oxygen-plasma treatment,[24] etching by superheated water in graphene nanobubbles[25] and by templating with SiO_2 fibers[26] or SiO_2 spheres.[27,28] To the best of our knowledge, none of these porous diamond materials were used in p-DSCs yet.

To address this point, we present here our initial results observed upon replacing the traditional flat diamond films from chemical vapor deposition (CVD) growth by so-called 'diamond foams'. This material was developed by Kato et al.[27] and was successfully tested for applications in double-layer supercapacitors.[27,28] It is grown by using SiO_2 spheres (500 nm in diameter) as templates, on which a thin BDD layer is deposited by standard CVD growth. The template is subsequently etched away by HF solution, leaving hollow spheres of diamond which replicate the SiO_2 template. The diamond-foam electrodes exhibit a relatively low specific capacitance (2.4-16 F/g) compared to e.g. activated carbon, but they are attractive because of their large electrochemical window and, particularly, because of their capability of fast charging at rates as high as 1000 V/s.[28]

3

To directly compare flat diamond films and diamond foams, we have functionalized the diamond foams with the same dyes as applied in our previous work on flat BDD films ('flat' means here a polycrystalline CVD-grown film which was deposited on a smooth substrate, such as a fused quartz plate[16,19]). More specifically, two different molecules were used as the diamond sensitizers, viz. (*E*)-2-{4-[2-(6-bromo-4,4-diethyl-4*H*-cyclopenta[1,2-*b*:5,4-*b*']dithiophen-2-yl)vinyl]-3-cyano-5,5-dimethylfuran-2(5*H*)-ylidene}malononitrile (coded **CPDT-Fur**) and (*Z*)-2-{5-[(5'-bromo[2,2'-bithiophen]-5-yl)methylene]-4-oxo-2-thioxothiazolidin-3-yl} acetic acid (coded **BT-Rho**). These molecules were anchored by the Suzuki coupling protocol through a phenyl linker, which was attached to the originally H-terminated diamond surface by diazonium electrografting.[19] The structures of the modified diamond surfaces are shown in Scheme 1.

Scheme 1 Structures of the chemically modified diamond surfaces with (a) **CPDT-Fur** and (b) **BT-Rho** sensitizers covalently anchored through a phenyl linker.

4

2. EXPERIMENTAL SECTION

2.1. Preparation and characterization of the BDD samples

Polycrystalline flat BDD thin films (150 nm in thickness) were grown by microwave plasma-enhanced chemical vapor deposition (MWCVD) from methane/hydrogen mixtures (1% CH_4) in an ASTeX 6500 reactor. The substrate was silicon or fused silica (1×1 cm^2). The substrate temperature was 700–900 °C, gas flow 500 sccm, total pressure 40 mbar, microwave power 3500 W. Trimethylborane gas was added during the growth with a ratio of 10000 ppm B/C to CH_4. This ratio corresponds to a boron concentration of ca. 10^{21} atoms/cm^3.[19] The sheet resistance, measured by a four-point probe, was 207 Ω/sq. Prior to the diamond growth, the substrates were cleaned for 15 min each in RCA 1 (30% NH_3 + 30% H_2O_2 + H_2O; 1:1:5) and RCA 2 (37% HCl + 30% H_2O_2 + H_2O; 1:1:5) solutions at 90 °C. Subsequently, the substrates were seeded with a nanodiamond dispersion in water. After deposition, the diamond samples were allowed to cool down in the reactor for 30 min under vacuum. To remove graphitic carbon, the as-deposited diamond films were boiled in 96% H_2SO_4 + 30% HNO_3 (3:1) at 90 °C for 30 min. After rinsing and sonicating with deionized water, the diamond samples were subjected to hydrogenation. This was performed using the same reactor (ASTeX 6500) under the following conditions: i) 500 sccm hydrogen flux, 40 mbar pressure with a 3500 W microwave power for 2 min, ii) 500 sccm hydrogen flux, 20 mbar pressure with a 2500 W microwave power for 5 min, iii) at the end of the plasma treatment, the microwave power was switched off and the samples were allowed to cool down under hydrogen flux for 1 hour.

The diamond foam was synthesized as described before.[28] Briefly, silica spheres (0.5 μm in diameter; Kisker Biotech GmbH & Co. Germany) were spin-coated from an isopropanol suspension onto a BDD diamond wafer (grown with the MWCVD method; 2 % CH_4 in H_2, 3200 W, 50 mbar, 750 °C, B/C = 4000 ppm). Subsequently, the spheres were seeded with aqueous 1 wt% H-terminated nanodiamond colloid and dried. BDD coating on the spheres was performed by the MWCVD method (1 % CH_4 in H_2; 2200 W, 40 mbar, 650 °C, B/C=12000 ppm). Typically, 5-6 layers of diamond-coated spheres on top of a compact BDD film were prepared. The electrode was then cleaned by boiling in H_2SO_4 + HNO_3 (3:1) for 1.5 h at 200 °C followed

by treatment with HF to remove the SiO_2 templates and finally rinsed with water and methanol. Before dye anchoring, the diamond foam was hydrogenated under the following conditions: i) 500 sccm hydrogen flux, 40 mbar pressure with a 3500 W microwave power for 5 min, ii) 500 sccm hydrogen flux, 20 mbar pressure with a 2500 W microwave power for 15 min, iii) at the end of the plasma treatment, the microwave power was switched off and the samples were allowed to cool down under hydrogen flux for 1 hour. (A longer treatment time was used for the foam than for the flat films to secure complete hydrogenation.) SIMS analysis of a one-layer electrode indicated a B-concentration of $(7-10) \cdot 10^{19}$ atoms/cm^3 for the foam layer and $\approx 10^{21}$ atoms/cm^3 for the supporting compact BDD film (cf. Fig. S1 in ESI).

2.2. Dye synthesis and surface anchoring

The two used dyes (**BT-Rho** and **CPDT-Fur**) were synthesized as outlined in our earlier work.[19] Commercially available chemicals were purchased in their purest grade and used as received. Sodium nitrite, sodium carbonate, sodium acetate, cesium acetate, cesium fluoride, potassium phosphate, palladium(II) acetate, 4-aminophenylboronic acid pinacol ester, rhodanine-3-acetic acid, tetrakis(triphenylphosphine)palladium(0), and tri(*o*-tolyl)phosphine were obtained from Sigma-Aldrich. 5-Bromo-5'-formyl-2,2'-bithiophene was acquired from TCI Europe N.V. 2-Dicyclohexylphosphino-2',6'-dimethoxybiphenyl (SPhos) was obtained from Acros Organics. The **CPDT-Fur** dye exhibits an extinction coefficient (ε) of 73100 M^{-1}cm^{-1} at λ = 582 nm.[19] The frontier orbital energy levels were determined from the oxidation and reduction onsets as observed by cyclic voltammetry (CV): E_{HOMO} = -5.70 eV and E_{LUMO} = -4.30 eV.[19] The corresponding values for **BT-Rho** are: ε = 43200 M^{-1}cm^{-1} at λ = 473 nm (UV-Vis spectrum in CH_2Cl_2 solution); E_{HOMO} = -5.91 eV and E_{LUMO} = -3.58 eV.

The functionalization of the diamond surface started with diazonization of the targeted aniline (4-aminophenylboronic acid pinacol ester) followed by electrochemical reduction of the *in situ* generated diazonium salt.[12,19] More specifically, 5 mM of 4-aminophenylboronic acid pinacol ester was diazotized with an equimolar amount of $NaNO_2$ in a (N_2 gas purged) 0.5 M HCl solution, which was directly used for CV scanning between +0.5 and -0.8 V (vs. Ag/AgCl) at a rate of 100 mV/s for 5 scans. After the modification, the substrate was sequentially rinsed and sonicated in water, THF and *n*-hexane. The Suzuki cross-coupling reaction was performed in a

6

glove box. A 15 mL ACE pressure tube (Sigma Aldrich) containing a magnetic stirring bar and the functionalized diamond film was charged with the dye, Pd catalyst, base and solvent and heated at 80 °C for 18 h. An optimized base/solvent/catalyst was used, as described elsewhere.[19]

2.3. Characterization methods

Scanning electron microscopy (SEM) images were obtained by a Hitachi FE SEM S-4800 microscope. The layer thickness was measured by profilometry (Dektak 150, Veeco). Raman spectra were measured with excitation by the 458 and 488 nm lines of an Ar^+/Kr^+ laser or the 633 nm line of a He-Ne laser, and recorded by a Labram HR spectrometer (Horiba Jobin-Yvon) interfaced to an Olympus microscope (objective 100x). UV-Vis absorption spectra were recorded with an Agilent Cary 500 Scan UV-Vis-NIR spectrometer in a continuous run from 200 to 800 nm at a scan rate of 600 nm min^{-1}. Secondary ion mass spectroscopy (SIMS) analysis was carried out using a SIMS 4500 (Cameca, USA). The surface was sputtered by oxygen ions accelerated at 5 kV. Adsorption isotherms of krypton (Kr) at 77 K were measured with a Micromeritics ASAP 2020 instrument (Micromeritics, Norcross, GA) on the supported thin-film electrodes. Following the usual practice, the saturation vapor pressure p_0 of supercooled liquid krypton and the atomic cross-sectional area of 0.21 nm^2 were used for data processing.[29,30]

Electrochemical experiments were carried out in a one-compartment cell using an Autolab PGstat-302N controlled by GPES-4 software. The BDD film was used as a working electrode (Ag contact with Au wire insulated by TorrSeal epoxy coating), platinum mesh was used as the counter electrode and a Ag/AgCl electrode (sat. KCl) was applied as the reference electrode. All electrochemical measurements were performed under Ar atmosphere. For the photoelectrochemical experiments, the cell was equipped with a quartz optical window, and the electrode was illuminated by a white light source (Oriel Xenon lamp, model 6269). The solar radiation (direct and diffuse) was simulated by an Oriel AM 1.5 Global (81088) filter. The light intensity was measured by a standard Si photodiode (PV Measurements, Inc. USA). For the quantum efficiency measurements (IPCE), the light was monochromatized using a Newport ¼ m grating monochromator (model 77200). Photoelectrochemical measurements were performed in an Ar-saturated 0.1 M Na_2SO_4 solution containing 5 mM methyl viologen (MV^{2+}), pH≈7. The counter electrode was platinum and the reference electrode was Ag/AgCl (sat. KCl). The

photoelectrochemical cell was placed in a dark room and controlled by a potentiostat (micro-AutolabIII, Ecochemie, B.V.) with NOVA software.

3. RESULTS AND DISCUSSION

3.1. Basic non-electrochemical characterization of the diamond foam electrodes

The SEM image of a flat BDD film (Fig. 1 top left) confirms the morphology of polycrystalline diamond. The foam electrodes are composed from spheres which are about 500 nm in size and are uniformly covered by diamond nanocrystals (Fig. 1). Occasionally, partly damaged spheres can be detected, which contain smaller or larger holes in the diamond shell. They were presumably created during dissolution of the SiO_2 templates. Sometimes, largely disintegrated structures with open hemispheres surrounded by debris material are observed, too. Damaged structures are more frequently observed in the dye-sensitized foam (see Fig. S2 in ESI).

Raman spectra of the BDD foam electrodes are shown in Fig. S3 (ESI). In accordance with previous works,[27,28] the sp^3-carbon (diamond) peak is detected at ca. 1330 cm^{-1}. The main impurity signals are assigned to *trans*-polyacetylene (1150 cm^{-1}) and to graphite-like (sp^2) carbon, which manifests itself by a broad and strong G-peak at ca. 1500 cm^{-1}. The absence of Raman features around 500 cm^{-1} indicates removal of SiO_2 as well as low B-doping. The latter is further confirmed by negligible Raman intensity near 1225 cm^{-1} where the Raman feature assigned to a Fano resonance line-shape of the diamond band normally occurs for heavily doped diamond.[31] The dye anchoring causes no marked changes to the Raman spectra (Fig. S3). For comparison, Raman spectra of flat BDD films on SiO_2 or Si substrates and with different excitation wavelengths are shown in Figs S4a and S4b (ESI). Again, no significant difference between pure and dye-sensitized films is observed. The strong features around 500 and 1200 cm^{-1} confirm larger B-doping of the flat films. The frequency of the first peak is known to scale with acceptor concentration which allows determination of the doping level.[32] The calculated concentration is $2 \cdot 10^{21}$ atoms/cm^3 which is near the expected value for the flat films (see Experimental Section). The diamond foam has a smaller dopant concentration by one order of

8

magnitude: $(7\text{-}10)\cdot 10^{19}$ atoms/cm^3 (as found by SIMS, see above). Furthermore, the signal of sp^2-carbon impurity is considerably smaller on the flat diamond compared to the diamond foam

Kr adsorption isotherms at 77 K were evaluated by the Brunauer-Emmett-Teller (BET) method. This procedure is applicable for determination of the roughness factor (R_f).[29,30] The detection limit of our method is about 20 in the R_f units[33] which is above the assumed values of R_f for flat diamond ($\approx$4, see Section 3.2). On the other hand, our BDD foam electrode provided good isotherm (Fig. S5; ESI) from which the R_f equals 114.
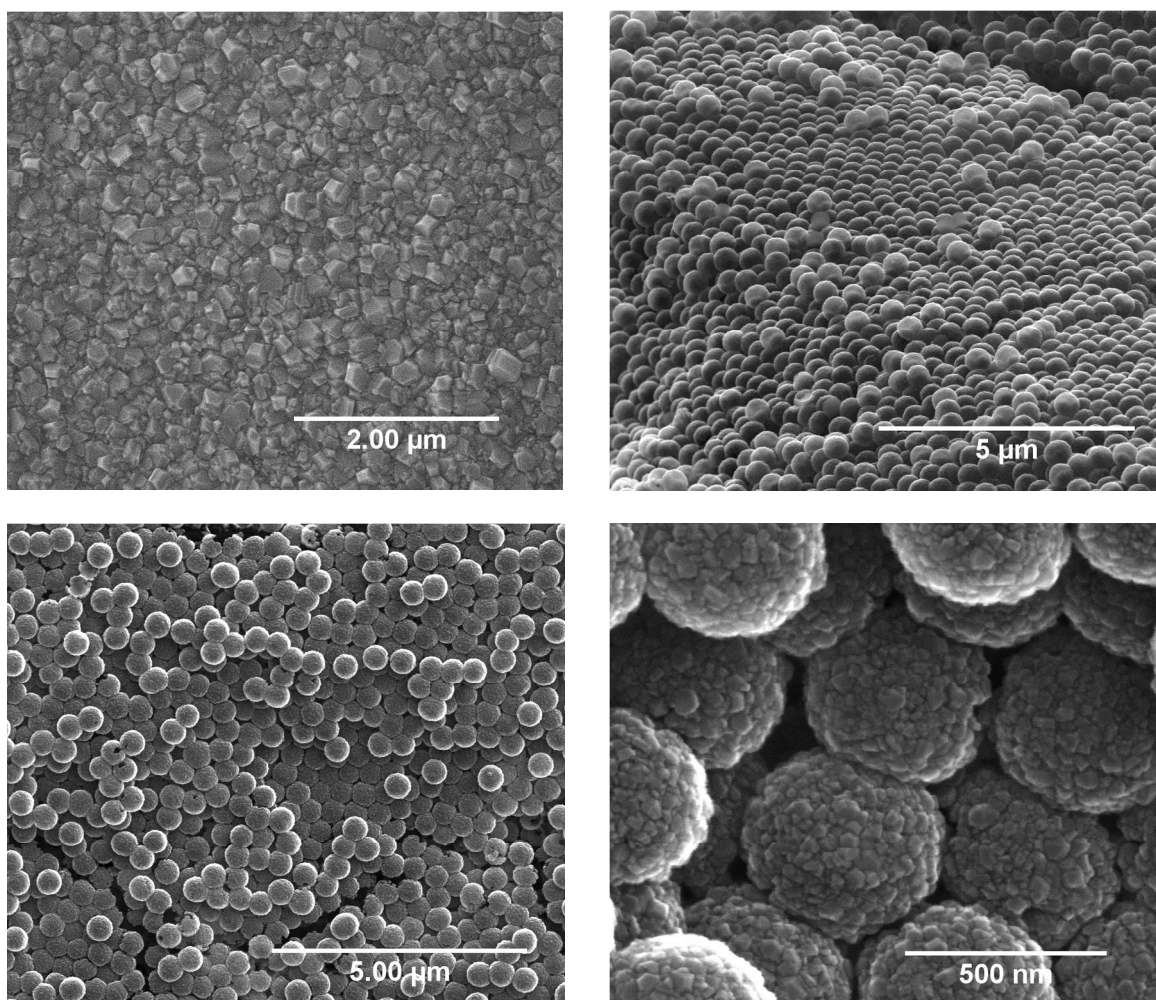

Fig. 1 SEM images of a compact BDD film (top left) and BDD foam electrodes (remaining images).

9

3.2. Electrochemistry (in dark)

Cyclic voltammetry of a blank BDD foam electrode in aqueous or aprotic electrolyte solution shows solely the capacitive-like voltammogram over a broad potential window.[27,28] This behavior is not significantly changed upon dye sensitization. The double layer capacitance, C can be calculated from the voltammetric current and the scan rate[16,34]:

$$i = dQ/dt = C\, dE/dt = Cv, \tag{1}$$

where Q is the voltammetric charge and dE/dt = v is the scan rate. The capacitance C of flat polycrystalline films is about 7-11 $\mu F/cm^2$[16,19,34,35] which is near the literature value for a single crystal diamond surface (ca. 3 $\mu F/cm^2$).[6] Hence, the roughness factor (R_f) of polycrystalline flat BDD films is estimated to be ca. 4. This is far below the usual roughness factor of nanocrystalline titania films ($R_f \approx 1000$) which are used in good DSCs of this kind[1]. The actual capacitance (R_f value) of a diamond foam sample obviously depends on the film thickness. A simple calculation of geometrical enlargement (f_{SE}) of cubic close packing of spheres gives[28]:

$$f_{SE} = \frac{4\pi}{\sqrt{3}} N \tag{2}$$

where N is the number of layers of closely-packed spheres. Our films are multilayers as demonstrated also by the SEM images (cf. Fig. S2, top-right chart). For $N = 5$ (see Experimental Section) we calculate $f_{SE} = 36.3$, which provides a crude estimate of $R_f \approx 145$, assuming the parent polycrystalline film has an intrinsic roughness factor of 4 (see above). This value is comparable to the experimentally found $R_f = 114$ from the Kr-adsorption isotherm (see Fig S5 and discussion thereof). The double-layer capacitance of our pristine BDD foam electrode, as measured by cyclic voltammetry at slower scan rates (<1 V/s), equals ca. 290 $\mu F/cm^2$ (Eq. 1 and Fig. S6 in ESI). This translates into $R_f \approx 97$, if we use the capacitance of single-crystal diamond as a reference. It should be noted, however, that the voltammetric double-layer capacitance is strongly dependent on the scan rate, due to limited transport of solvated ions in the porous structure.[28] Hence, the lower R_f values from electrochemistry, compared to those from Kr-

adsorption, are understandable. The relative increase of R_f between flat film and foam is about 25. As the dye coverage is known to be close to monolayer on flat films (about 0.6 ML for both dyes [19]) we can estimate its enhancement by a factor of ≈25 on the foam in an ideal case.

We further measured the cyclic voltammograms of the diamond electrodes (both flat films and foams) in the electrolyte solution, which was applied in the photoelectrochemical experiments (5 mM methyl viologen in 0.1 M Na_2SO_4, pH 7; see below). Fig. 2 shows the relevant data with a reference voltammogram obtained on an indium-tin oxide (ITO) electrode. The latter exhibits the expected redox waves of methyl viologen (redox potential of -0.65 V vs. Ag/AgCl)[36]. On a flat diamond electrode, these waves become highly irreversible, although the electrochemical responsiveness of BDD to methyl viologen is known to be quite good[37]. Interestingly, the sensitized BDD flat film exhibits a total blocking of the MV^{2+}/MV^+ redox couple. This may indicate that reduction of our dyes requires more negative potentials than the reduction of MV^{2+} as indicated by the positions of the E_{LUMO} levels (see Experimental Section). This hypothesis is supported for **BT-Rho**, while **CPDT-Fur** has a reduction potential near that of methyl viologen.

The voltammetric response of the diamond foam electrodes is interestingly different. In contrast to the flat BDD film, the pristine foam shows quasi-reversible waves of the MV^{2+}/MV^+ redox couple like on ITO. The redox-blocking by the dyes is again seen, albeit it is not as perfect as on the flat films. We ascribe both effects to the presence of sp^2-carbon impurities (graphite and *trans*-polyacetylene; see Fig. S3 and discussion of Raman spectra) which do not anchor dyes, and presumably to incomplete dye coverage of the hollow diamond spheres as shown in Figs. 1 and S2. Fig. 2 (dashed color curves) further shows the voltammograms of sensitized electrodes, which passed the long-term photoelectrochemical test (several hours of chopped illumination with white light under negative bias). These voltammograms are discussed below.
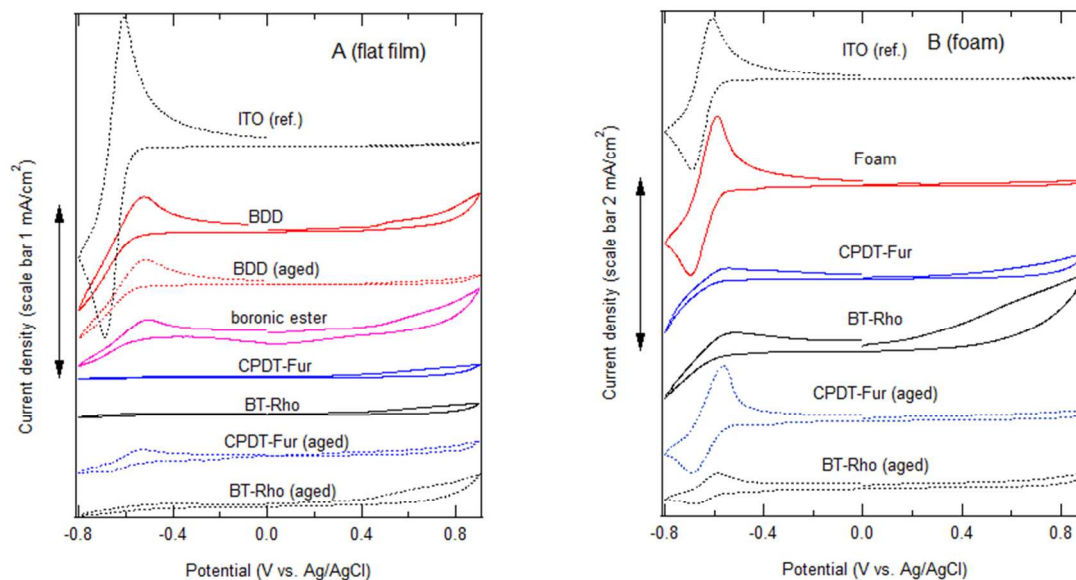
11

Fig. 2 Cyclic voltammograms in 0.1 M Na$_2$SO$_4$ + 5 mM methyl viologen; scan rate 100 mV/s. **(A) Flat BDD film**. From top to bottom: pure ITO (reference), pure BDD film, BDD film after ca. 40 hours of photoelectrochemical aging (see below), BDD film modified by boronic ester (synthetic intermediate), fresh BDD film sensitized with **CPDT-Fur**, fresh BDD film sensitized with **BT-Rho**, BDD film sensitized with **CPDT-Fur** after photoelectrochemical aging, BDD film sensitized with **BT-Rho** after photoelectrochemical aging. **(B) Diamond foam.** From top to bottom: pure ITO (reference), pure foam, fresh foam sensitized with **CPDT-Fur**, fresh foam sensitized with **BT-Rho**, **CPDT-Fur** sensitized foam after photoelectrochemical aging, **BT-Rho** sensitized foam after photoelectrochemical aging. Curves are offset for clarity, but the scale is identical for all plots in the respective chart.

3.3. Photoelectrochemistry

Fig. 3 shows the response of a sensitized diamond foam at experimental conditions similar to those used in our earlier work.[19] It surveys the behavior of freshly made electrodes during the first 6 minutes of their testing at chopped illumination by white light (20 mW/cm^2). We observed cathodic photocurrent densities of ca. 500-700 nA/cm^2 at -0.2 V bias for a foam electrode sensitized with both **CPDT-Fur** and **BT-Rho**. The occurrence of a cathodic photocurrent is a consequence of hole injection from the photoexcited dye into the valence band of BDD.[9,12-16,19] More specifically, light excitation generates electron-hole pairs in the sensitizer molecule.

12

Subsequently, the exciton dissociates thanks to the donor-π-bridge-acceptor molecular structure of **CPDT-Fur** and **BT-Rho** (Scheme 1). Then, the separated electrons flow to the MV^{2+} (methyl viologen) electron carrier in the electrolyte solution and holes are injected into the BDD. The HOMO levels of the dyes (-5.7 eV and -5.9 eV for **CPDT-Fur** and **BT-Rho,** respectively – see Experimental Section) are below the valence band of H-terminated diamond (which is ca. -4.2 eV for diamond in vacuum, and ca. -5.5 eV for a diamond contacting electrolyte solution).[6] This energy difference provides the necessary driving force for hole injection.

The observed photocurrent densities on diamond foam are approximately 3-times larger than those on flat diamond, if we take into account the different light intensities in the reference work.[19] However, that the photocurrent density is not enhanced proportionally to the increase of R_f, as it follows from the surface area enlargement (Section 3.2.). This is likely due to incomplete dye coverage, which is caused by the presence of sp^2 impurities and the complicated morphology of our foam electrodes. (Incomplete dye coverage on the foam is also corroborated by the partial dislodging of the MV^{2+}/MV^+ redox reaction, see Fig. 2 and discussion thereof).
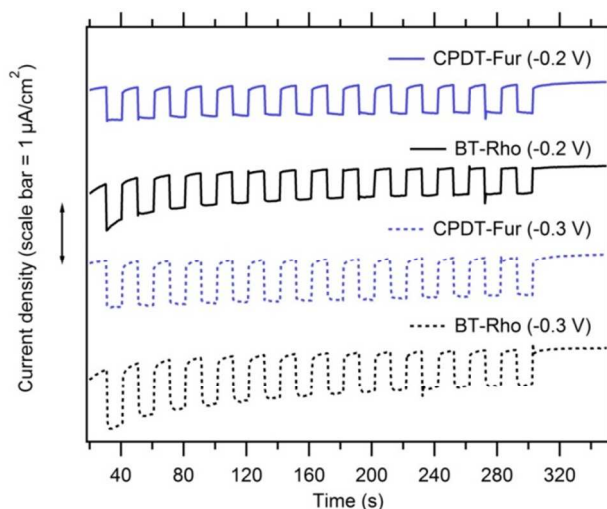

Fig. 3 Chronoamperometric measurements of a fresh diamond foam sensitized with **CPDT-Fur** or **BT-Rho**. Electrolyte solution: 5 mM methyl viologen in 0.1 M Na_2SO_4, pH 7. The applied bias voltage (vs. Ag/AgCl) is indicated in annotations. Chopped white light illumination (20 mW/cm^2; simulated AM 1.5G solar spectrum).

To investigate the long-term stability of the electrodes, we have repeated the experiment as in Fig. 3, but on a larger timescale and with a 5-times larger light intensity (100 mW/cm^2; 1 sun). The corresponding plot is shown in Fig. 4 for the **BT-Rho** sensitizer. The response of the BDD foam electrode sensitized with **CPDT-Fur** was similar (Fig. S7, ESI).
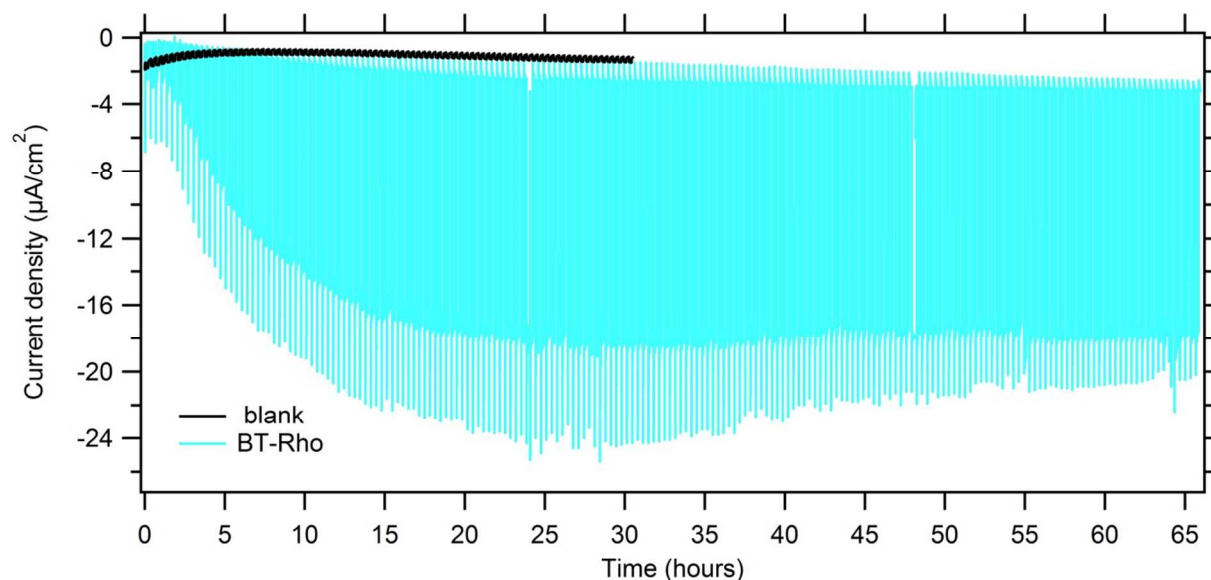

Fig. 4 Long-term chronoamperometric measurement of the diamond foam electrode sensitized with **BT-Rho**. For comparison, the same plot for a blank (non-sensitized) diamond foam is also shown. Chopped white light illumination (100 mW/cm^2; simulated AM 1.5G solar spectrum, 10 min dark/light interval). Electrolyte solution: 5 mM methyl viologen in 0.1 M Na$_2$SO$_4$, pH 7; applied potential: -0.3 V vs. Ag/AgCl.

The blank (sensitizer-free) foam shows stable photocurrent densities of ca. 300 nA/cm^2 at these conditions (light intensity, bias; see black curve in Fig. 4). Cathodic photocurrent densities of ca. 5-10 nA/cm^2 were previously reported for a blank (non-sensitized) BDD electrode with flat surface and ca. 10-times smaller light intensity.[16,19] Figure S8 (ESI) compares our pristine foam and flat electrodes. Under the applied experimental conditions (white light of 20 mW/cm^2 power and bias of -0.3 V), the foam exhibits a stable cathodic photocurrent of 50-60 nA/cm^2, while the flat diamond delivers ca. 20 nA/cm^2. Interestingly, we observe a factor of ≈3 enhancement for

the foam (as for the sensitized photocurrent, but this might be just a coincidence). The cathodic photocurrent under sub-bandgap illumination of blank BDD has been ascribed to either sp^2 carbon impurities or to specific states related to B in the lattice.[38] In spite of its unclear origin, the onset of the cathodic photocurrent transients scales with pH and the flatband potential of BDD.[38] We should note that the diamond foam indeed contains a significant proportion of sp^2 carbon impurities (*trans*-polyacetylene and graphitic carbon)[27,28] (cf. Fig. S3).

The most striking effect, observed in both Figs 4 and S7 is the huge enhancement of photocurrent simply when the chopped illumination progresses for hours. After 1 day of this 'aging-activation', the photocurrent density on the **BT-Rho** sensitized foam (which was initially ca. 2 $\mu A/cm^2$ for the fresh electrode) increased to ca. 15 $\mu A/cm^2$ (Fig. 4). Our champion electrode exhibited a maximum photocurrent density of about 22 $\mu A/cm^2$; the corresponding plot is shown in Fig. S9 (ESI). Furthermore, sharp current transients are observed at the light on/off events, which were missing in the fresh samples (Fig. 3). The on/off current transients are often observed on dye-sensitized semiconductor electrodes and are attributed to sluggish charge-transport kinetics, in particular to slow diffusion of the molecules of the electrolyte redox-mediator (MV^{2+} in our case).[1] The absence/occurrence of current spikes in Figs. 3 and 4, respectively, can be simply attributed to the different time scales of both experiments. This is illustrated in Fig. S10 (ESI), showing that the current spikes in Fig. 4 develop during ca 50 s, which is longer than the time interval of light on/off switching used in Fig. 3.

To the best of our knowledge, the observed photocurrent densities of 15-22 $\mu A/cm^2$ at 1 sun illumination are the largest, among all values for sensitized diamond electrodes previously reported.[9,12-16,19] This remarkable photoelectrochemical activity is ascribed to the unique morphology of the diamond foam electrodes with an enhanced surface area for light-harvesting.

Details of the above-described 'aging-activation' were further explored for electrodes at various stages of the photoelectrochemical treatment. Fig. 5 shows the plots for the **BT-Rho** sensitized foam electrode. The corresponding plot for the **CPDT-Fur** foam electrode is similar (Fig. S11 in ESI). Again, the current transients are not expressed when the light chopping is fast (10 s dark/light). For the aging-activated electrodes, the photocurrent density scales linearly with the

15

light intensity (between 0.1 and 1 sun, as shown in Figs 5 and S11). The effect of applied voltage is illustrated in Fig. S12 (ESI) for an aged **BT-Rho** electrode. As expected,[16,19] the photocurrent density increases with negative bias.
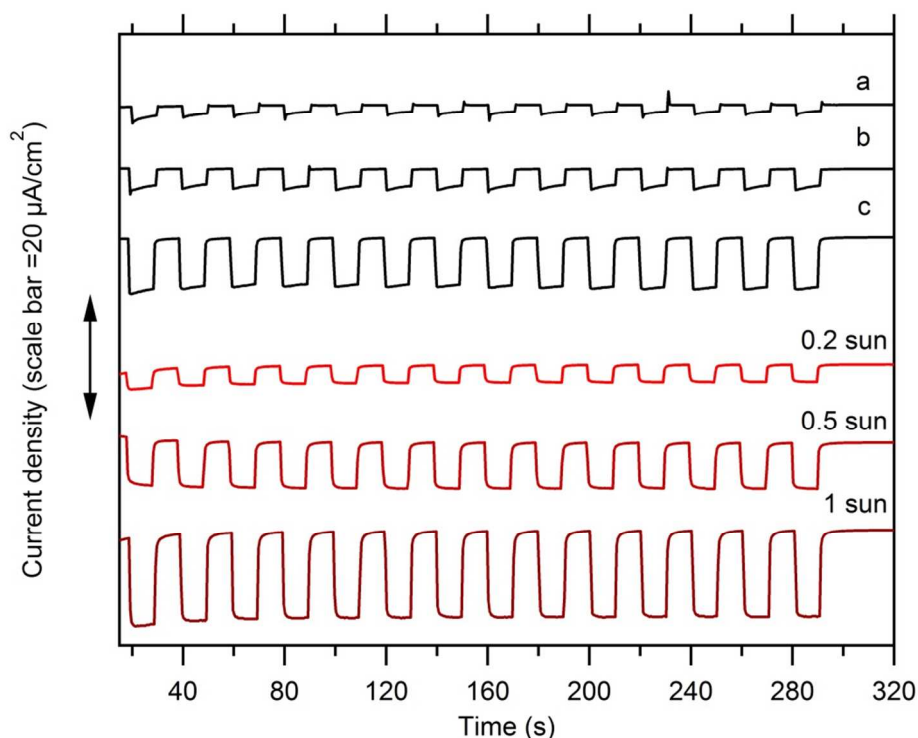

Fig. 5 Chronoamperometric measurement of a diamond foam electrode sensitized with **BT-Rho**. Chopped white light illumination (simulated AM 1.5G solar spectrum). Electrolyte solution: 5 mM methyl viologen in 0.1 M Na_2SO_4. Applied potential bias: -0.2 V vs. Ag/AgCl. Curves from top to bottom: (a) fresh electrode, 1 sun, (b) the same electrode after several tens of minutes at 1 sun, (c) the same electrode after ca. 5 hours at 1 sun. Red curves are for measurements after ca. 50 hours with different light intensities.

We further explored the question whether or not the photoelectrochemical 'aging-activation' is specific for the diamond foam only. To this purpose, the long-term behavior of the sensitized flat BDD films was analyzed as well. The samples were identical to those investigated in our earlier paper.[19] Fig. S13 (ESI) presents an example of a **BT-Rho**-modified flat diamond film. The

photocurrent density increase is again obvious. This confirms that the photoelectrochemical 'aging activation' is not specific for the diamond foam, but it occurs on the flat films, too.

To further explore the effect of 'aging-activation' we measured the action spectra (IPCE vs. wavelength) at various stages of activation (Fig. 6). IPCE is defined by the equation:

$$IPCE = \frac{i_{ph} h \nu}{Pe} \qquad (3)$$

where i_{ph} is the photocurrent density, h is Planck's constant, ν is the photon frequency, P is the incident light power and e is electron charge. For a flat sensitized surface, the maximum accessible $IPCE$ is the product of the quantum yield of hole injection (or electron injection in the case of n-type semiconductors) from the photoexcited dye, η_{inj} and the light-harvesting efficiency, which is given by the dye's extinction coefficient ε and the dye's surface coverage Γ.

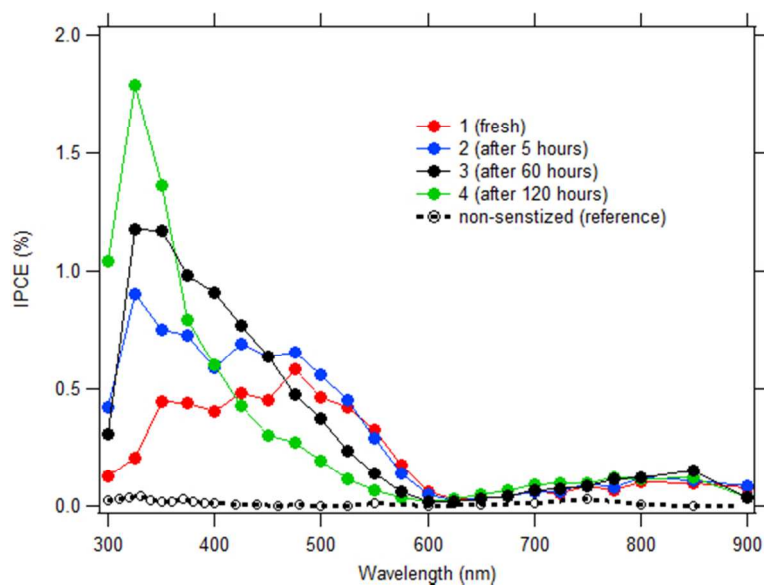$$IPCE = \eta_{inj} (1-10^{-\Gamma\varepsilon}) \qquad (4)$$

Fig. 6 IPCE spectra for a diamond foam electrode sensitized with **BT-Rho**: (1) at the beginning of the experiment, (2) after 5 hours, (3) after 60 hours, (4) after 120 hours of chopped illumination at 1 sun intensity. A reference spectrum for pristine, non-sensitized foam is also shown. Electrolyte solution: 0.1 M Na$_2$SO$_4$ + 5 mM methyl viologen, pH 7; applied bias -0.3 V vs Ag/AgCl.

17

The IPCEs and photocurrent densities observed in this study are better than those, previously achieved for sensitized BDD electrodes.[9,12-16,19] The blank (non-sensitized) foam expectedly shows negligible IPCEs over the whole spectral region studied from UV to near-IR. The fresh sensitized electrode exhibits an IPCE/wavelength spectrum which resembles the UV-Vis optical spectrum of the fresh **BT-Rho** dye. The pure dye has a main absorption peak at 445 nm and a second weaker one at 320 nm (in ethanolic solution), but the spectrum shows significant changes upon illumination with white light at 1 sun intensity (Fig. S14a in ESI). The main visible peak attenuates, and the UV peak broadens toward shorter wavelengths. Similar spectral changes are observed also for a thin film of the **BT-Rho** dye (Fig. S14b in ESI). The observed spectral variations resemble those of the IPCE/wavelength spectra upon aging (Fig. 6).

The maximum IPCEs gradually increase and shift towards the UV part of the spectrum. Qualitatively, this leads to a hypothesis that the structure of the dye and/or diamond-dye surface complex is changing, but an in-depth analysis of these structural changes and their effect on photocurrent generation is beyond the scope of this paper. We only note that the electrochemical properties of the dye-sensitized electrodes change too, upon aging. As discussed in Section 3.2. (Fig. 2), the aged electrodes were considerably more active towards the MV^{2+}/MV^{+} redox couple as compared to the response of fresh sensitized diamonds. This effect is particularly expressed for the foam electrodes. However, the physical interpretation of the aging-activation of the dye-sensitized diamond surface is unclear, and it will be addressed by refined analytical and structural studies in the near future.

4. CONCLUSIONS

Diamond foam, composed of hollow spheres of polycrystalline B-doped diamond, was used for spectral sensitization with two donor-π-bridge-acceptor dyes, **BT-Rho** and **CPDT-Fur**. These molecular dyes were covalently anchored to the diamond surface through a phenyl linker. Chemical modification of the diamond surface was performed through a combination of diazonium electrografting and Suzuki cross-coupling reactions. The prepared materials were

tested as electrodes in the dark and upon illumination in an aqueous electrolyte solution with methyl viologen acting as a reversible electron acceptor. Reference experiments were carried out with standard flat BDD films.

Chemical derivatization of the flat diamond surface by **BT-Rho** and **CPDT-Fur** caused a complete blocking of the methyl viologen (MV^{2+}/MV^+) redox reaction, whereas the redox-blocking effect was less perfect for the sensitized foam electrodes. This is ascribed to the presence of sp^2-carbon impurities, such as *trans*-polyacetylene and graphite-like carbon, which are detected by Raman spectroscopy. Cathodic photocurrent densities of ca. 500-700 nA/cm^2 were observed at -0.2 V bias for a fresh foam electrode sensitized with both **CPDT-Fur** and **BT-Rho** illuminated by white light (20 mW/cm^2; simulated AM 1.5G solar spectrum). These photocurrent densities are approximately 3 times larger than those on flat diamond, which is attributed to the enhanced surface area of the foam electrodes.

Long-term (1-2 days) illumination of the sensitized foam electrodes with chopped white light at 1 sun intensity and -0.3 V bias caused a significant increase of cathodic photocurrent densities to values of ca. 15-22 $\mu A/cm^2$. These are the largest photocurrent densities reported so far for dye-sensitized diamond electrodes. The photocurrent densities scale linearly with light intensity (between 0.1 a 1 sun). The activation is accompanied with characteristic changes of the dark voltammogram of the MV^{2+}/MV^+ redox couple and with gradual changes of the IPCE spectra. The latter initially resemble the optical UV-Vis absorption spectrum of the dye, but subsequently the maximum IPCEs increase and shift towards the UV. The photoelectrochemical 'aging-activation' is expressed also on flat diamond films, but detailed physical interpretation of the effect remains elusive.

ACKNOWLEDGEMENT

Electronic Supplementary Information (ESI): SIMS and Raman spectra of diamond foam electrodes, Kr-adsorption isotherm, UV-Vis spectra, additional SEM images and electrochemical data.

References

1. A. Hagfeldt, G. Boschloo, L. Sun, L. Kloo and H. Pettersson, *Chem. Rev.* 2010, **110**, 6595.

2. S. Mathew, A. Yella, P. Gao, R. Humphry-Baker, B.F.E. Curdoch, N.A. Astani, I. Tavernelli, U. Rothlisberher, M.K. Nazeeruddin and M. Grätzel, *Nature Chem.* 2014, **6**, 242.

3. H. Tian, J. Oscarsson, E. Gabrielsson, S.K. Eriksson, R. Lindblad, B. Xu, Y. Hao, G. Boschloo, E.M.J. Johansson, J.M. Gardner, A. Hagfeldt, H. Rensmo and L. Sun, *Sci. Rep.* 2014, **4**, 4282.

4. S. Powar, T. Daeneke, M.T. Ma, D. Fu, N.W. Duffy, G. Goetz, M. Weidelener, A. Mishra, P. Baeuerle, L. Spiccia and U. Bach, *Angew. Chem. Int. Ed.* 2013, **52**, 602.

5. A. Nattestad, A.J. Mozer, M.K.R. Fischer, Y.B. Cheng, A. Mishra, P. Bäuerle and U. Bach, *Nature Mat.* 2010, **9**, 31.

6. Fujishima, A., Einaga, Y., Rao, T. N., and Tryk, D. A., *Diamond Electrochemistry*, Elsevier, Tokyo,, 2005.

7. L. Kavan, Z. Vlckova-Zivcova, V. Petrak, O. Frank, P. Janda, H. Tarabkova, M. Nesladek and V. Mortet, *Electrochim. Acta* 2015, **doi:org/10.1016/j.electacta.2015.04.124**.

8. C.H.Y.X. Lim, Y.L. Zhong, S. Janssens, M. Nesladek and K.P. Loh, *Adv. Funct. Mater.* 2010, **20**, 1313.

9. Y.L. Zhong, A. Midya, Z. Ng, Z.K. Chen, M. Daenen, M. Nesladek and K.P. Loh, *J. Am. Chem. Soc.* 2008, **130**, 17218.

10. S.D. Janssens, P. Pobedinskas, J. Vacik, V. Petrikova, B. Ruttens, J. D'Haen, M. Nesladek, K. Haenen and P. Wagner, *New. J. Phys.* 2011, **13**, 083008.

11. S. Mori, S. Fukuda, S. Sumikura, Y. Takeda, Y. Tamaki, E. Suzuki and T. Abe, *J. Phys. Chem. C.* 2008, **112**, 16134.

12. Y.L. Zhong, K.P. Loh, A. Midya and Z.K. Chen, *Chem. Mater.* 2008, **20**, 3137.

13. C. Petkov, U. Glebe, E. Petkov, A. Pasquarelli, C. Pietzka, M. Veres, L. Himics, R. Merz, W. Kulisch, U. Siemeling, J.P. Reithmaier and C. Popov, *Phys. Stat. Sol. A* 2013, **210**, 2048.

14. J. Bechter, C. Pietzka, C. Petkov, P. Reintanz, U. Siemeling, C. Popov and A. Pasquarelli, *Phys. Stat. Sol. (a)* 7-1-2014, **211**, 2333.

15. W.S. Yeap, X. Liu, D. Bevk, A. Pasquarelli, L. Lutsen, M. Fahlman, W. Maes and K. Haenen, *ACS Appl. Mat. Interfaces* 2014, **6**, 10322.

16. H. Krysova, Z. Vlckova-Zivcova, J. Barton, V. Petrak, M. Nesladek, M. Cigler and L. Kavan, *Phys. Chem. Chem. Phys.* 2015, **17**, 1165.

17. P. Qin, H. Zhu, T. Edvinsson, G. Boschloo, A. Hagfeldt and L. Sun, *J. Am. Chem. Soc.* 2008, **130**, 8570.

18. P. Qin, J. Wiberg, E.A. Gibson, M. Linder, L. Li, T. Brinck, A. Hagfeldt, B. Albinsson and L. Sun, *J. Phys. Chem. C* 2010, **114**, 4738.

19. S.W. Yeap, D. Bevk, X. Liu, H. Krysova, A. Pasquarelli, D. Vanderzande, L. Lutsen, L. Kavan, M. Fahlman, W. Maes and K. Haenen, *RSC Adv.* 2014, **4**, 42044.

20. L. Kavan, M. Grätzel, S.E. Gilbert, C. Klemenz and H.J. Scheel, *J. Am. Chem. Soc.* 1996, **118**, 6716.

21. L. Kavan, *Chem. Rec.* 2012, **12**, 131.

22. F. Gao, R. Thomann and C.E. Nebel, *Electrochem. Comm.* 2015, **50**, 32.

23. F. Gao and C.E. Nebel, *Phys. Stat. Sol. (a)* 2015, **DOI 10.1002/pssa.201532131**.

24. C. Terashima, K. Arihara, S. Okazaki, T. Shichi, D.A. Tryk, T. Shirafuji, N. Saito, O. Takai and A. Fujishima, *ACS Appl. Mat. Interfaces* 2011, **3**, 177.

25. C.H.Y.X. Lim, A. Sorkin, Q. Bao, A. Li, K. Zhang, M. Nesladek and K.P. Loh, *Nature Comm.* 2013, **4**, 1556.

26. M.K. Singh, E. Titus, J.C. Madaleno, G. Cabral and J. Gracio, *Chem. Mater.* 2008, **20**, 1725.

27. H. Kato, J. Hees, R. Hoffmann, M. Wolfer, N. Yang, S. Yamasaki and C.E. Nebel, *Electrochem. Comm.* 2013, **33**, 88.

28. F. Gao, M.T. Wolfer and C.E. Nebel, *Carbon* 2014, **80**, 833.

29. J. Prochazka, L. Kavan, V. Shklover, M. Zukalova, O. Frank, M. Kalbac, A. Zukal, H. Pelouchova, P. Janda, K. Mocek, M. Klementova and D. Carbonne, *Chem. Mater.* 2008, **20**, 2985.

30. J. Prochazka, L. Kavan, M. Zukalova, O. Frank, M. Kalbac, A. Zukal, M. Klementova, D. Carbonne and M. Grätzel, *Chem. Mater.* 2009, **21**, 1457.

31. P.W. May, W.J. Ludlow, M. Hannaway, P.J. Heard, J.A. Smith and K.N. Rosser, *Diamond Rel. Mater.* 2008, **17**, 105.

32. Z. Vlckova-Zivcova, V. Petrak, O. Frank and L. Kavan, *Diamond Rel. Matter.* 2015, **55**, 70.

33. J. Prochazka, L. Kavan, M. Zukalova, P. Janda, J. Jirkovsky, Z. Vlckova-Zivcova, A. Poruba, M. Bedu, M. Dobbelin and R. Tena-Zaera, *J. Mater. Res.* 2013, **28**, 385.

34. Z. Vlckova-Zivcova, O. Frank, V. Petrak, H. Tarabkova, J. Vacik, M. Nesladek and L. Kavan, *Electrochim. Acta* 2013, **87**, 518.

35. J. Scharpf, A. Denisenko, C. Pietzka and E. Kohn, *Diamond Rel. Mater.* 2011, **20**, 1250.

36. L. Kavan, N. Tetreault, T. Moehl and M. Grätzel, *J. Phys. Chem. C* 2014, **118**, 16408.

37. Y. Show, M.A. Witek, P. Sonthalia and G.M. Swain, *Chem. Mater.* 2003, **15**, 879.

38. S.J. Green, L.S.A. Mahe, D.R. Rosseinsky and C.P. Winlove, *Electrochim. Acta* 2013, **107**, 111.

TOC Graphic

CPDT-Fur

BT-Rho

Diamond foam

500 nm

23